

See discussions, stats, and author profiles for this publication at: <https://www.researchgate.net/publication/333719432>

# control-systems-principles.co.uk

Technical Report · June 2019

DOI: 10.13140/RG.2.2.14965.83686

CITATIONS

0

READS

365

2 authors, including:



[Mark Christopher Readman](#)

Stockprt College/Trafford College Group

24 PUBLICATIONS 113 CITATIONS

[SEE PROFILE](#)

Some of the authors of this publication are also working on these related projects:



Nonlinear Control [View project](#)

## Coupled Drives 2: Control and analysis

Mark Readman, Hilde Hagadoorn, control systems principles.co.uk

**ABSTRACT:** This is one of a series of white papers on systems modelling, analysis and control, prepared by Control Systems Principles.co.uk to give insights into important principles and processes in control. In control systems there are a number of generic systems and methods which are encountered in all areas of industry and technology. These white papers aim to explain these important systems and methods in straightforward terms. The white papers describe what makes a particular type of system/method important, how it works and then demonstrates how to control it. The control demonstrations are performed using models of real systems designed by our founder and senior partner Peter Wellstead, and have been developed for manufacture by TQ Education and Training Ltd in their CE range of equipment. This white paper uses the computer based control and simulation tool CE20000 together with the coupled drives CE108.

### 1. Introduction

The coupled drive experiment is a multivariable system designed to demonstrate speed and tension control. As described in the first white paper, two motors are connected to a jockey pulley with a belt that acts as a flexible coupling. Dynamic coupling between the two drive motors and the jockey pulley is due to the drive belt. By varying the speed of the motors the vertical position and the rotational speed of the jockey pulley can be controlled. Belt driven systems are used extensively in the automotive industry together with passive and active tension control. Tension and speed control is also an important issue in the paper and steel industries. Normally in these areas tension is controlled by varying the web speed at different locations. The manufactured paper or steel acts like a flexible belt. Control of vibration is also an important issue in high performance belt driven power trains and an ongoing topic of research.

The first coupled drives white paper (see [www.control-systems-principles.co.uk](http://www.control-systems-principles.co.uk) and go to the downloads page), described the background and dynamics of the coupled drives process. In this white we are going to describe the dynamics from a difference way and do a series of experiments with the CE108 equipment. The CE2000 software is used to investigate closed-loop control of the coupled drive system. This is a multivariable control problem and will demonstrate the use of a precompensator to decouple the open-loop dynamics into two Single Input Single Output (SISO) transfer functions. This allows SISO design methods to be applied to the tension and speed loops.

These control exercises are illustrated in the video clips on the control systems principles web site

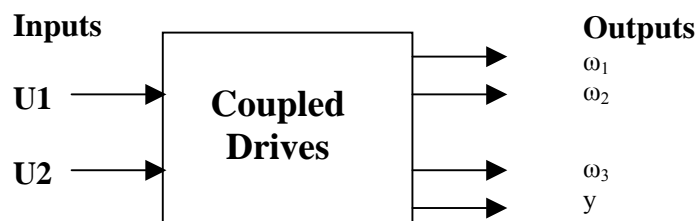


**Figure 1. Coupled Drives Block Diagram**

In the above block diagram  $\omega_{1,2}$  are the motor speeds and  $\omega_3$  is the jockey pulley speed and  $y$  is the tension output. We will also look at multivariable speed control where the objective is to independently control the speed of each motor.

## 2. Dynamic Equations

The Newton/Euler dynamic equations for the coupled drive system are developed in the white paper

<http://www.control-systems-principles.co.uk/coupled-drives-system.pdf>

Here we show an alternative way of developing the dynamic equations based on Lagrangian techniques [1]. The notation used here will follow the above white paper. Nominal values of the units shown are used to obtain simulated results.

### Notation (units and nominal values in brackets)

$\theta_{1,2}$	Motor <sub>1,2</sub> angular position (rad)
$\theta_3$	Jockey pulley angular position (rad)
$\omega_{1,2}$	Motor <sub>1,2</sub> pulley angular velocity (rad/sec)
$\omega_3$	Jockey pulley angular velocity (rad/sec)
$x$	Jockey pulley linear position (m)
$I_{1,2}$	Motor <sub>1,2</sub> inertia (8e-4 kg m <sup>2</sup> )
$I_3$	Jockey pulley inertia (4e-4 kg m <sup>2</sup> )
$m$	Jockey pulley mass (0.35 kg)
$r$	Radius all pulleys (0.03 m)
$k$	Belt stiffness (50 Nm <sup>-1</sup> )
$k_0$	Jockey spring stiffness (200 Nm <sup>-1</sup> )
$b_{1,2}$	Motor friction (9e-2 Nms <sup>-1</sup> )
$b_3$	Pulley friction (angular 1e-3 Nms <sup>-1</sup> )
$b_m$	Pulley friction (translation 0.5 Ns <sup>-1</sup> )
$\alpha$	Angle (rad)

First we write down expressions for the kinetic energy, potential energy and dissipation and assemble the Lagrangian. Next we use Lagranges equations to obtain the dynamics. A figure of the coupled drives is shown in the above white paper.

### Kinetic Energy

Note in the following analysis the jockey pulley drive inertia  $I_3$  is assumed to be zero and the mass of the drive belt is assumed to be zero. With these assumptions the kinetic energy for the system is

$$T = \frac{1}{2}m\dot{x}^2 + \frac{1}{2}I_1\dot{\theta}_1^2 + \frac{1}{2}I_2\dot{\theta}_2^2 \quad (1)$$

## Potential Energy

From the kinematic relationship between the jockey pulley position and the belt shown in Figure 2, the following expression for potential energy is obtained.

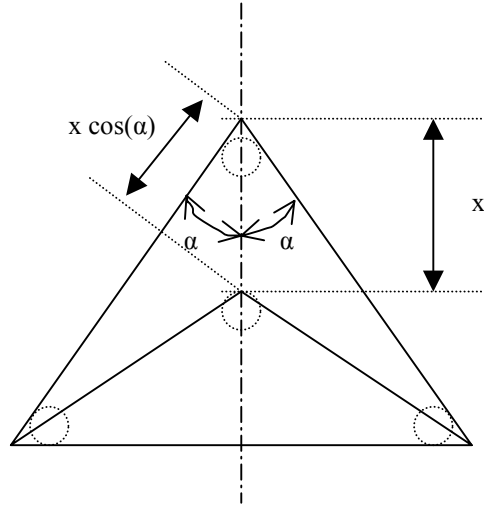


**Figure 2. Calculation of Potential Energy**

$$V = \frac{1}{2}k[r(\theta_1 - \theta_2)]^2 + \frac{1}{2}k[r(\theta_1 - \theta_3) - x \cos(\alpha)]^2 + \frac{1}{2}k[r(\theta_3 - \theta_2) - x \cos(\alpha)]^2 + \frac{1}{2}k_0x^2 \quad (2)$$

With the assumption

$$\theta_3 = \frac{\theta_1 + \theta_2}{2} \quad (3)$$

the expression for potential energy simplifies to,

$\therefore$

$$V = \frac{1}{2}k[r(\theta_1 - \theta_2)]^2 + k\left[\frac{r}{2}(\theta_1 - \theta_2) - x \cos(\alpha)\right]^2 + \frac{1}{2}k_0x^2 \quad (4)$$

## Dissipation

Here we only consider dissipation due to the drive motors and the jockey pulley mass.

$$R = \frac{1}{2}b_1\dot{\theta}_1^2 + \frac{1}{2}b_2\dot{\theta}_2^2 + \frac{1}{2}b_0\dot{x}^2 \quad (5)$$

The jockey pulley friction  $b_3$  is assumed to be zero.

### Lagrangian

The Lagrangian is obtained in the usual manner

$$L = T - V \quad (6)$$

### Dynamic Equations

We now obtain the dynamic equations using,

$$\begin{aligned} \frac{d}{dt} \frac{\partial L}{\partial \dot{\theta}_i} - \frac{\partial L}{\partial \theta_i} + \frac{\partial R}{\partial \dot{\theta}_i} &= u_i \quad i = 1, 2 \\ \frac{d}{dt} \frac{\partial L}{\partial \dot{x}} - \frac{\partial L}{\partial x} + \frac{\partial R}{\partial \dot{x}} &= 0 \end{aligned} \quad (7)$$

These equations can be written in the form

$$M \ddot{z} + B \dot{z} + K_s z = U \quad (8)$$

where

$$z = (\theta_1 \quad \theta_2 \quad x)^T \quad \text{and} \quad U = (u_1 \quad u_2 \quad 0)^T$$

$$M = \begin{pmatrix} I_1 & 0 & 0 \\ 0 & I_2 & 0 \\ 0 & 0 & m \end{pmatrix}, \quad B = \begin{pmatrix} b_1 & 0 & 0 \\ 0 & b_2 & 0 \\ 0 & 0 & b_0 \end{pmatrix}, \quad K_s = \begin{pmatrix} \frac{3}{2}kr^2 & -\frac{3}{2}kr^2 & -kr\cos(\alpha) \\ -\frac{3}{2}kr^2 & \frac{3}{2}kr^2 & kr\cos(\alpha) \\ -kr\cos(\alpha) & kr\cos(\alpha) & k_0 + 2k\cos^2(\alpha) \end{pmatrix} \quad (9)$$

Dynamic coupling between the drive motors and the jockey pulley position and rotation is due to the drive belt. This information is contained in the stiffness matrix  $K_s$ . So it is the stiffness matrix that provides the dynamic coupling in the dynamic equations.

$$\left. \begin{array}{l} 0^\circ \\ \alpha = 30^\circ \\ 90^\circ \end{array} \right\} = \begin{array}{l} \text{Max coupling} \\ \text{Coupled drives} \\ \text{Decoupled} \end{array}$$

For the coupled drives we take  $\alpha = 30^\circ$  so  $\cos(\alpha) = \sqrt{3}/2$  and the stiffness matrix becomes (actually  $\alpha(x,t)$  but we assume  $\alpha = \text{constant}$ )

$$K = \begin{pmatrix} \frac{3}{2}kr^2 & -\frac{3}{2}kr^2 & -\frac{\sqrt{3}}{2}kr \\ -\frac{3}{2}kr^2 & \frac{3}{2}kr^2 & \frac{\sqrt{3}}{2}kr \\ -\frac{\sqrt{3}}{2}kr & \frac{\sqrt{3}}{2}kr & k_0 + \frac{3}{2}k \end{pmatrix} \quad (10)$$

### Transfer functions

Writing the dynamic equations in the form (Note the inertia matrix  $M$  is positive definite and hence invertible)

$$\ddot{z} + M^{-1}B \dot{z} + M^{-1}K z = M^{-1}U \quad (11)$$

and using Laplace transforms we get

$$z(s) = G(s) U(s) \quad (12)$$

where

$$G(s) = (s^2 + M^{-1}B s + M^{-1}K)^{-1} M^{-1} \quad (13)$$

and the outputs are

$$z = (\theta_1 \quad \theta_2 \quad x)^T$$

The inputs can be written as

$$U(s) = \begin{pmatrix} 1 & 0 \\ 0 & 1 \\ 0 & 0 \end{pmatrix} \begin{pmatrix} u_1 \\ u_2 \end{pmatrix} = K_{in} \begin{pmatrix} u_1 \\ u_2 \end{pmatrix} \quad (14)$$

The outputs we are interested in are the jockey pulley angular velocity and tension. Jockey pulley angular position is defined in equation (3). By differentiating angular position we obtain angular velocity so we can write the output equation as

$$\begin{pmatrix} \omega_3 \\ x \end{pmatrix} = \begin{pmatrix} \frac{s}{2} & \frac{s}{2} & 0 \\ 0 & 0 & 1 \end{pmatrix} \begin{pmatrix} \theta_1 \\ \theta_2 \\ x \end{pmatrix} = K_{out} \begin{pmatrix} \theta_1 \\ \theta_2 \\ x \end{pmatrix} \quad (15)$$

and obtain the transfer function from motor input to jockey speed and tension

$$\begin{pmatrix} \omega_3 \\ x \end{pmatrix} = \begin{pmatrix} \frac{s}{2} & \frac{s}{2} & 0 \\ 0 & 0 & 1 \end{pmatrix} \begin{pmatrix} \theta_1 \\ \theta_2 \\ x \end{pmatrix} \quad (16)$$

so finally

$$\begin{pmatrix} \omega_3 \\ x \end{pmatrix} = P(s) \begin{pmatrix} u_1 \\ u_2 \end{pmatrix} \quad (17)$$

where

$$P(s) = K_{out} G(s) K_{in} = \begin{pmatrix} G_\omega & G_\omega \\ -G_x & G_x \end{pmatrix} = \begin{pmatrix} G_\omega & 0 \\ 0 & G_x \end{pmatrix} \begin{pmatrix} 1 & 1 \\ -1 & 1 \end{pmatrix} \quad (18)$$

and

$$G_\omega = \frac{1}{2(Is + b)} \quad (19)$$

$$G_x = \frac{\sqrt{3}kr}{(Is^2 + 3kr^2)(2ms^2 + 2k_0 + 3k) - 3k^2r^2}$$

Note the damping factors in the tension transfer function have been neglected for simplicity.

Also note that above calculations are more easily performed using a symbolic manipulation package such as DERIVE. The sensor gain matrix is approximately

$$K_{sen} = \begin{pmatrix} K_{speed} & 0 \\ 0 & K_{tension} \end{pmatrix} = \begin{pmatrix} 0.001 & 0 \\ 0 & 10 \end{pmatrix} \quad (20)$$

Using the variable values above gives the model dynamics and multiplying by the sensor gain gives

$$K_{sen} \begin{pmatrix} G_\omega & 0 \\ 0 & G_x \end{pmatrix} = \begin{pmatrix} \frac{1}{0.3s + 1} & 0 \\ 0 & \frac{-185600}{(s^2 + 11s + 150)(s^2 + 1.6s + 800)} \end{pmatrix} \quad (21)$$

### 3. Tension and Jockey speed control

Writing the coupled drives transfer function as shown in equation (22) suggests using a constant precompensator to decouple the jockey speed and tension dynamics.

$$\begin{pmatrix} \omega_3 \\ x \end{pmatrix} = \begin{pmatrix} G_\omega & 0 \\ 0 & G_x \end{pmatrix} \begin{pmatrix} 1 & 1 \\ -1 & 1 \end{pmatrix} \begin{pmatrix} u_1 \\ u_2 \end{pmatrix} \quad (22)$$

This allows the MIMO system to be treated as two SISO systems. Applying the pre-compensator

$$K(s) = \begin{pmatrix} 1 & -1 \\ 1 & 1 \end{pmatrix} \quad (23)$$

decouples jockey speed and tension so that the decoupled system becomes,

$$P(s)K(s) = \begin{pmatrix} \frac{1}{0.3s+1} & 0 \\ 0 & \frac{-185600}{(s^2+11s+150)(s^2+1.6s+800)} \end{pmatrix} \quad (24)$$

Both these transfer functions are stable but notice that a sign change has occurred in the tension dynamics. The block diagram in Figure 3. below shows the plant with decoupling pre-compensator. Now  $r_1(s)$  and  $r_2(s)$  are the control inputs and  $\omega_3(s)$  and  $y(s)$  are the jockey pulley speed and tension outputs respectively.

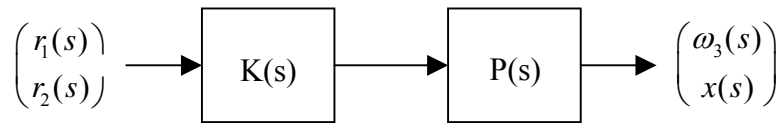


**Figure 3. Diagonalising Precompensator K(s)**

### Open-Loop Dynamics

In this experiment we first obtain the decoupled open-loop step response of the jockey speed and tension dynamics. This illustrates the use of a pre-compensator to decouple jockey speed from the tension control loop. The CE2000 program shown in Figure 3 is used for the open-loop experiments. To examine the decoupled jockey speed dynamics the tension input is set to zero and a square wave is applied to the speed input. This applies the same control signal to both motors. The nominal speed of the jockey pulley was set to  $-2.0$  Volts. The jockey speed output is the response to the square wave input while the tension output shows little interaction Figure 4.

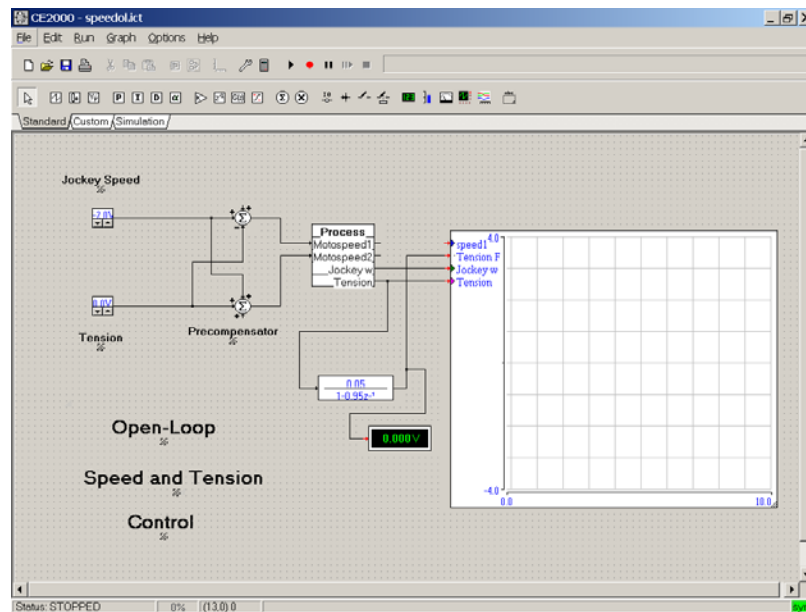


**Figure 4. Open-Loop Jockey Speed and Tension Testing**



To examine the decoupled tension dynamics the jockey speed input is set to a nominal  $-2.0$  Volts. A

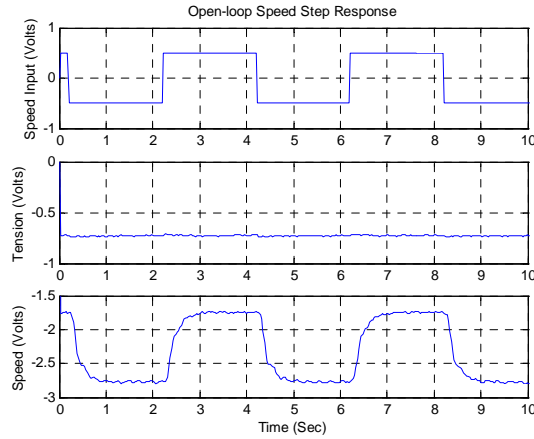


**Figure 5. Open-Loop Jockey Speed Step Response**

square wave is applied to the tension input. In Figure 5 we have shown the raw tension output and the filtered tension output. The lowpass filter

$$F(z) = \frac{1 - \beta}{1 - \beta z^{-1}} \quad (25)$$

is used to filter the raw tension data where  $\beta=0.95$ . Notice that in this case there is some interaction with the jockey speed. The tension dynamics contains a pair of under damped poles with natural frequencies of 25 and 18 rad/sec respectively.

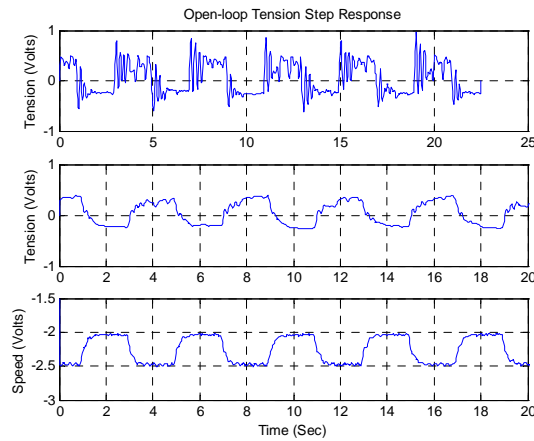


**Figure 6. Open-Loop Jockey Tension Step Response**

### Jockey Speed control

The decoupled transfer function can be approximated by the transfer function and controlled by a PI controller,

$$P(s) = \frac{1}{\tau s + 1} \quad \tau \approx 0.3$$

$$K_{\omega}(s) = K_p + \frac{K_i}{s}$$
(26)

The loop gain is

$$L(s) = P(s)K(s) = \frac{K_p s + K_i}{s(\tau s + 1)}$$
(27)

and the sensitivity and complementary sensitivity functions are

$$S(s) = \frac{1}{1 + L(s)} = \frac{s(s + \frac{1}{\tau})}{s^2 + \frac{(1 + K_p)}{\tau}s + \frac{K_i}{\tau}}$$

$$T(s) = L(s)S(s) = \frac{\frac{K_p}{\tau}(s + \frac{K_i}{K_p})}{s^2 + \frac{(1 + K_p)}{\tau}s + \frac{K_i}{\tau}}$$
(28)

The proportional and integral gains for jockey speed control can be tuned online. In this experiment the following values were chosen.

$$K_p = 1.0, \quad K_i = 5.0$$

Substituting the above values into the transfer function gives the closed-loop step dynamics

$$T(s) = \frac{3.33(s + 5)}{s^2 + 6.6676s + 16.67}$$

and step response shown in the Figure 6 below.

The position of the zero in the complementary sensitivity function  $T(s)$  can have a big effect on the

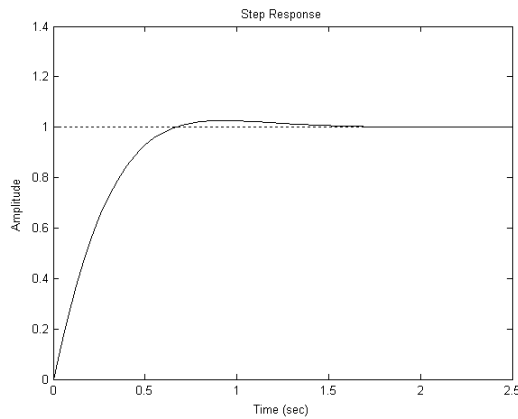


**Figure 7. Simulated Closed-Loop Jockey Speed Step Response**

transient response. See Dorf chapter 5 for details.

## Tension Control

From the model of the coupled drive system the nominal decoupled tension dynamics can be approximated by the transfer function,

$$P(s) = \frac{-185600}{(s^2 + 11s + 150)(s^2 + 1.6s + 800)} \quad (29)$$

This is a stable transfer function with two pairs of complex poles. There are a fast underdamped pair of poles with a natural frequency  $\sim 5\text{Hz}$  due to the jockey position, and a slow slightly under-damped pair of poles with a natural frequency of approximately  $2\text{Hz}$  due to rotational elastic coupling between the two motors and the jockey pulley. Note the actual natural frequencies of the pair of complex poles will depend on the actual version of the CE108 that is being used. The negative sign is the result of using the pre-compensator and affects the controller implementation. As with the jockey speed control we want the closed-loop tension dynamics to track a step change in the tension reference. A stable transfer function can always be made closed-loop stable by making the loop gain small enough (remember the small gain theorem). However, in this case to achieve closed-loop stability the controller gain has to be made quite small. Then the closed-loop response will be not much different to the open-loop response and the steady state error will be large. The steady state error can be removed by using an integral controller. This also

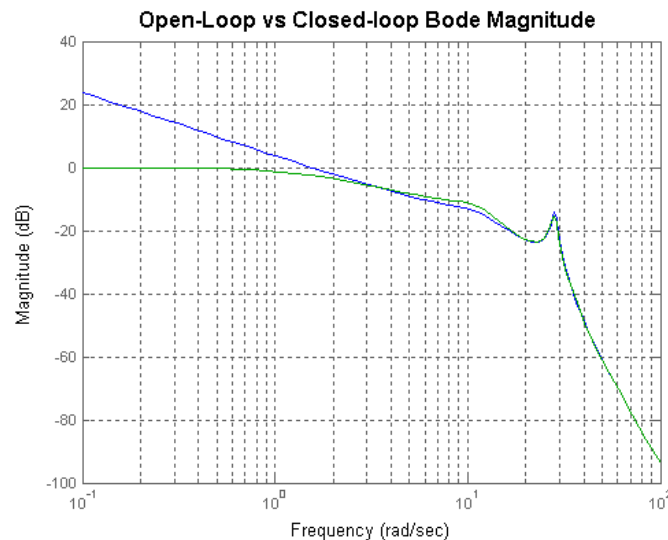


**Figure 8. A comparison of the loop gain  $L(s)$  and closed-loop gain  $T(s)$  when using integral control.**

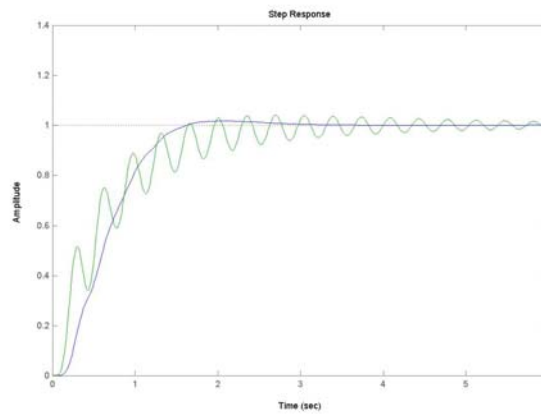
improves the stability margins by rolling off the loop gain well below the pole frequencies. A Bode magnitude plot comparing the open-loop gain with the closed-loop gain is shown in Figure 8. The closed-loop bandwidth of  $2\text{rad/sec}$  or  $0.3\text{ Hz}$  is approximately a decade below the smallest mode. A further increase in closed-loop robustness is obtained by rolling off the loop gain faster resulting in the following compensator where the pole time constant is  $\tau$ .

$$K_x(s) = \frac{K}{s(\tau s + 1)} \quad \tau \approx 0.4 \quad (30)$$

Assuming a sampling interval of  $T_s=50$  ms, the ZOH digital controller is

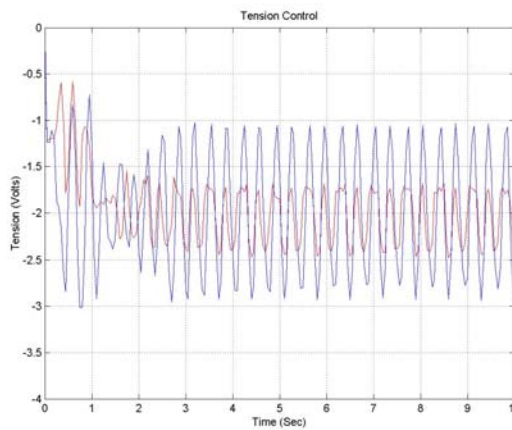
$$K_x(z) = \frac{0.003z^{-1} + 0.002876z^{-2}}{1 - 1.882z^{-1} + 0.8825z^{-2}} \quad (31)$$

Figure 8. is a simulation of the step response using the compensator shown above. For comparison also shown is the step response using integral control only. Notice that the additional lag improves the step response. The time constant in the low pass filter can be tuned to give best performance on a particular CE108.



**Figure 9. Simulated Closed-Loop Tension Step Response**

The next figure shows the transient response when the CE108 is started up. This compares the integral controller to the integral plus lag controller. The robust controller gives improved rejection of the periodic disturbance occurring at the chosen jockey pulley speed.



**Figure 10. Experimental Closed-Loop Transient Response**

## Experimental Results: Jockey Speed and Tension Control

Putting it all together, the pre-compensator  $K(s)$  is used decouple the jockey speed and jockey tension dynamics. Jockey speed is controlled using the speed controller  $K_\omega(s)$ , while the tension is controlled using the tension controller  $K_x(s)$  obtained in the previous section. Note, due to a sign change in the tension dynamics introduced by the pre-compensator the tension feedback loop is positive.

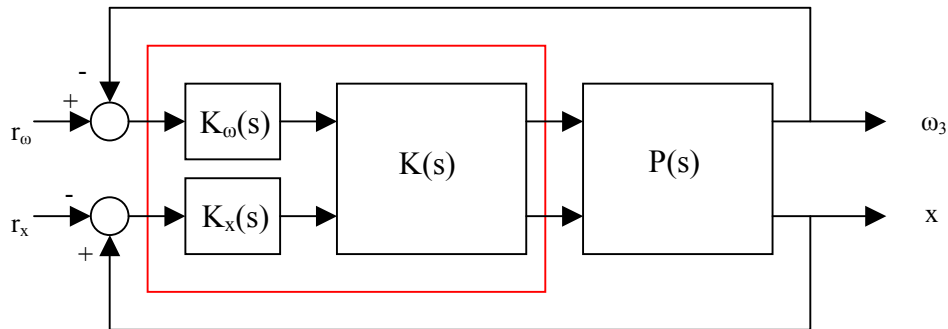


**Fig 11. Tension and Speed Control**

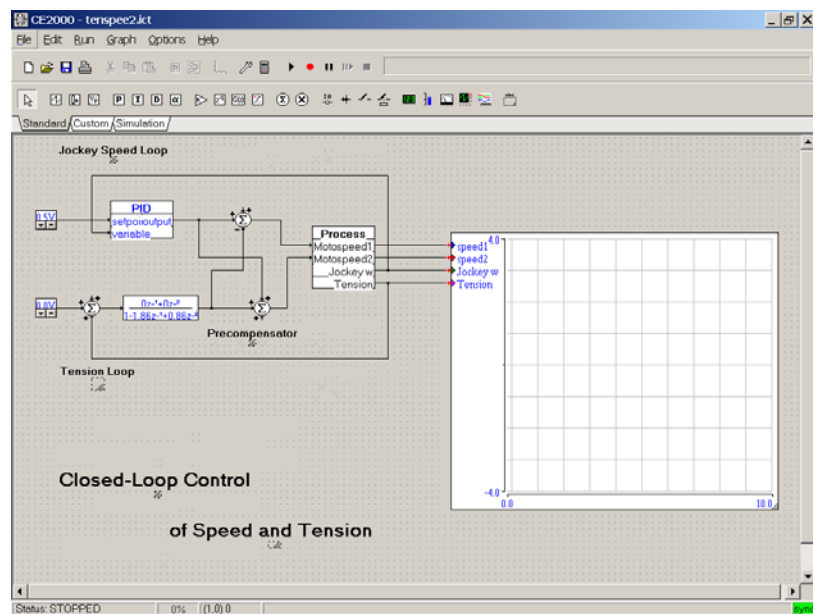


**Figure 12. CE2000 Program For Speed and Tension Control**

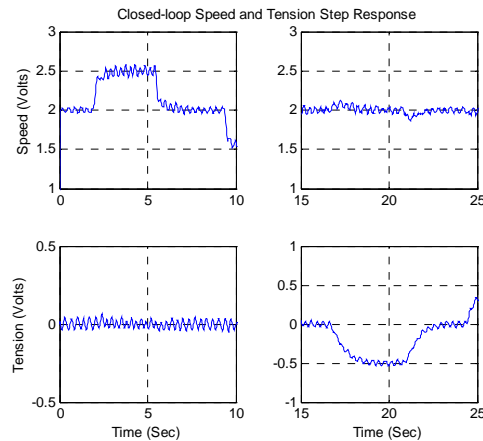


**Figure 13. Closed-Loop Tension and Speed Step Response**

### Controlling the fast tension dynamics

The tension control loop has fast dynamics. These were not controlled in the previous sections where the closed-loop bandwidth was kept below the natural frequency of the fast dynamics which were treated as an uncertainty. A more interesting problem is to examine how we can actively control the fast dynamics. To examine the fast tension dynamics we can initially displace the jockey pulley and examine the resulting transient response. This will allow us to estimate the natural frequency and damping ratio. Set the input to both motors to zero using the CE2000 program shown in Figure 3. Next depress the tension bar to until  $-2.0$  Volts is indicated on the tension sensor. Release the tension bar and record the resulting transient response. This transient response is shown in the above Figure. The dominant dynamics are underdamped with a frequency of approximately  $4.5\text{Hz}$  and a damping ratio of  $\zeta=0.1$ . These numbers are

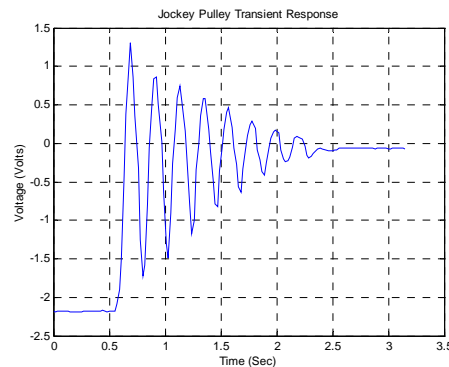


**Figure 14. Experimental Open-Loop Tension Dynamics**

only approximate and will be slightly different for each CE108 coupled drive. To control the tension will require a sampling time of around  $10\text{ms}$ .

#### 4. Motor Speed Control

In this section we show experimentally that it is possible to independently control the speed of the two motors. This is interesting because this is not possible using the model obtained in the previous sections. Due to symmetry the transfer function from motor inputs to motor speed outputs does not have full rank and therefore the model cannot be decoupled using feedback or a precompensator. A block diagram of the system is shown below.

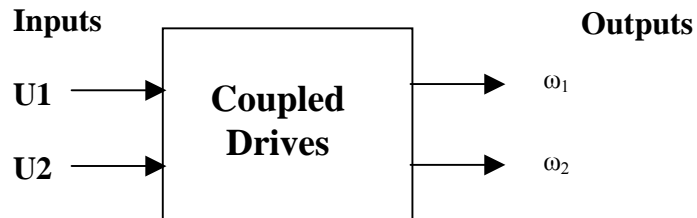


Figure 15. Speed Control

In the experiment independent PI controllers used to control the speed of each motor. As in the previous section a pre-compensator can be introduced to reduce interaction between motor speeds.

#### Open-Loop Speed Dynamics

To examine the open-loop speed dynamics both motor inputs are set to a nominal voltage of 3 Volts. The input voltages are alternatively toggled by  $\pm 1.0$  Volt. The Figures below shows the output voltages for motor 1 (blue), motor 2 (green) and the jockey pulley speed (red). In this experiment the motors and the

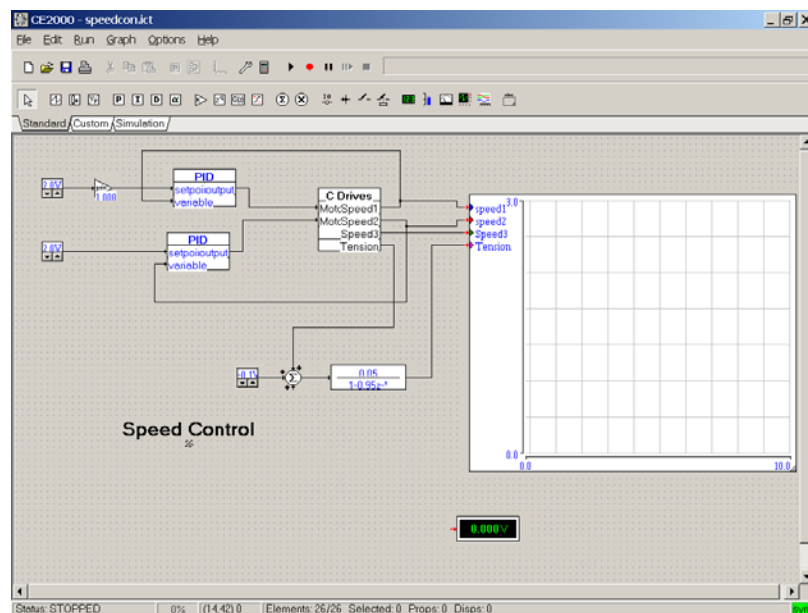
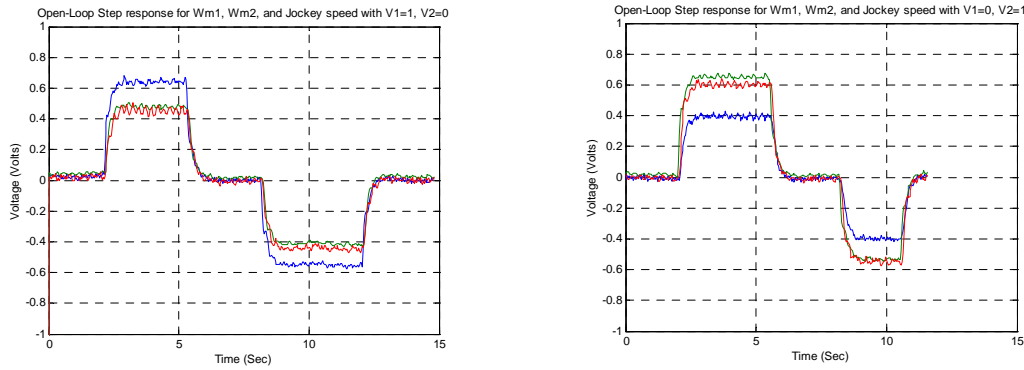


Figure 16. CE2000 Program For Speed Control

belt rotate clockwise. After passing over the jockey pulley the belt passes over motor 2. Note that the jockey pulley speed tracks motor 2 speed and not that average of the two speeds as predicted by the model. If the belt direction is reversed then the after passing over the jockey the pulley passes over motor 1. The jockey pulley speed will track motor 1 speed.



**Figure 17. CE108 Open-Loop Speed Step Response**

A section of the step response is shown in the figure below. This allows us to estimate the following simple model for the two speed outputs.

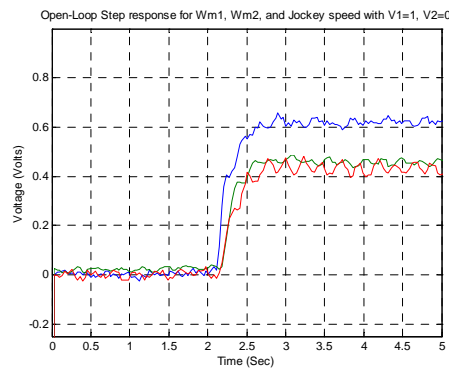


**Figure 18. Step Response**

$$\begin{pmatrix} \omega_1(s) \\ \omega_2(s) \end{pmatrix} = P(s) \begin{pmatrix} u_1(s) \\ u_2(s) \end{pmatrix} \quad (32)$$

$$P(s) = \begin{pmatrix} 0.6 & 0.4 \\ 0.4 & 0.6 \end{pmatrix} \frac{1}{(0.5s + 1)} \quad (33)$$



## Multivariable Speed Control

In this section we demonstrate multivariable speed control using the coupled drives. The objective is to independently control the speed of each motor. To do this a PID controller

$$C(s) = K_p + \frac{K_i}{s} \quad (34)$$

is used to control the speed of each motor. The nominal reference speed of both motors is set to 2 Volts. The figure below shows the closed-loop step response when a step of 0.5 Volts is applied to motor 1. After a small initial disturbance the speed of motor 2 is maintained close to 2 Volts while the speed of motor 1 follows the reference input to 2.5 Volts. Similarly when the reference input to motor 2 is 2.5 Volts motor 2 the speed of motor 2 follows the reference while the speed of motor 1 is maintained close to the reference voltage.

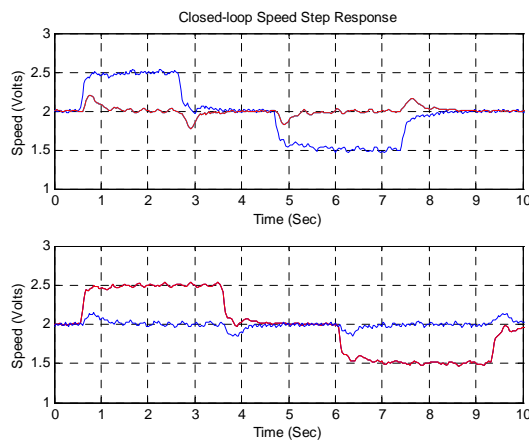


**Figure 19. Experimental Closed-Loop Speed Control**

## 5. A Final Word

It is not possible to answer questions about our white papers, unless we have a contract with your organisation. For more information about the CE2000 Control and Simulation Software go to the TQ Education and Training web site using the links on our web site [www.control-systems-principles.co.uk](http://www.control-systems-principles.co.uk) or use the email [info@tq.com](mailto:info@tq.com). There are many books and tutorial papers that will help you with the theoretical background of control for the coupled drives, we are particularly indebted to the references listed below. For a web search of references, try key words such as coupled drives and tension control, belt drives and dancer.

## 6. References

1. Wellstead P. E Introduction To Physical Modelling Systems, Academic Press 1979
2. Dorf, R C and Bishop, R H, Modern Control Systems, (9<sup>th</sup> Ed) Prentice Hall 2000.
3. Readman, M. C, Flexible Joint Robots, CRC Press, 1994
4. Torkel Glad and Lennart Ljung, Control Theory Multivariable and Nonlinear Methods, Taylor and Francis 2000.
5. <http://www.control-systems-principles.co.uk/coupled-drives-system.pdf>